Paper

Theoretical Evaluation of Spectral Power Distributions of Radiant Energy from Microcavities

Seishi SEKINE , Masatoshi UENO , Hiroaki SUZUKI and Masashi OHKAWA

Department of Electrical and Electronic Engineering
Faculty of Engineering, Niigata University
Ikarashi 2-8050, Niigata 950-2181, Japan

Received Dec. 17, 1997

ABSTRACT

Characteristics of radiation from microcavities are investigated to verify the luminous efficacy of microcavity radiator that was estimated by John F. Waymouth in 1989. Electromagnetic waves in a rectangular microcavity and a cylindrical microcavity were analyzed based on the waveguide theory. The modes of electromagnetic waves in the microcavities are analyzed using a normalized eigenfunction. The conductivity and permittivity of metals are obtained by analyzing the motion equation of the free electron in the metals. The skin depth of tungsten is estimated with the emissivity of tungsten based on electromagnetic theory. Accordingly it is estimated that the luminous efficacy of radiation from the microcavity is expected to reach 118 lm/W.

1. Introduction

At the 5th International Light Source Symposium in 1989 at York, England, John F. Waymouth proposed a method for reducing the emissivity of tungsten in the infrared wavelengths, thereby increasing the luminous efficacy of incandescent tungsten[1]. The method was achieved by patterning the surface of tungsten with sub-micron-wide and several micron-deep microcavities. Waymouth estimated that this surface configuration can potentially increase the luminous efficacy to 60 - 80 lm/W at filament temperatures of only 2000 to 2100 K. Since then several experimental studies to test this Waymouth Hypothesis have been conducted by other researchers[2,3]. The dramatic potential predicted that was by this hypothesis, however, has not necessarily been demonstrated by those studies.

Therefore, to verify the Waymouth Hypothesis, we studied the spectral power distributions of radiant energy on the surface of tungsten with microcavities.

We analyzed

(1) the modes of electromagnetic waves in the microcavities with the perfect conductor based on the theories of waveguide,
(2) the modes of electromagnetic waves in the microcavities with walls of imperfect conductors based on the theories of cavity resonator,
(3) the skin depth of tungsten, and obtained
(4) the spectral power distributions in the microcavities,
(5) spectral radiant emittance from the microcavities.

This paper reports on results of these analysis and characteristics of radiation from the microcavities.

2. Electromagnetic Field of the Microcavities and that of the Cavity Walls

We considered microcavities with which the surface of a tungsten radiator is patterned. Even if the cavity is not vacuous, but filled with rare gases such as argon and halogen, the electromagnetic waves within the cavities can be practically regarded as that in a vacuum.

When the electromagnetic waves vibrate with the frequency of v as simple harmonic motions, the angular frequency ω is defined as $\omega = 2\pi v$. For electric field strength, $\mathbf{E}$, and magnetic field strength, $\mathbf{H}$, of the electromagnetic waves, Maxwell's fourth equation in the cavities is

$$\nabla \times \mathbf{H} = j\omega\varepsilon_0\mathbf{E}, \quad \nabla^2\mathbf{E} + k^2\mathbf{E} = 0, \ k^2 = \omega^2\mu_0\varepsilon_0, \tag{1}$$

where μ_0 and ε_0 are the permeability and permittivity of free space, respectively, and on the cavity walls:

$$\nabla \times \mathbf{H} = (\sigma + j\omega\varepsilon)\mathbf{E}, \quad \nabla^2\mathbf{E} + \tilde{k}^2\mathbf{E} = 0, \ \tilde{k}^2 = \omega^2\mu(\varepsilon - j\sigma/\omega), \tag{2}$$

where μ, ε and σ are the permeability, permittivity and conductivity of the cavity walls, respectively.

3. The Modes of Electromagnetic Waves in the Microcavities

3.1 The Microcavities of Rectangular Waveguide

As shown in Fig.1, in the microcavity of square waveguide that has four walls at $y = 0, L$ and $z = 0, L$, we considered the electromagnetic waves traveling in the direction +x. The x−component of **E**, E_x, which is the TM waves, is given by

$$E_x = E_{0x}\sin k_y y \sin k_z z e^{-jk_x x}, \qquad (3)$$

and that of **H**, H_x, which is the TE waves, is given by

$$H_x = H_{0x}\cos k_y y \cos k_z z e^{-jk_x x}, \qquad (4)$$

where

$$k^2 = k_x^2 + k_y^2 + k_z^2, \quad k_y = m\pi/L, k_z = n\pi/L, \qquad (5)$$

and parameters m and n are positive integers. The wave number k is defined as $k = 2\pi/\lambda$ on the wavelength of electromagnetic waves, λ.

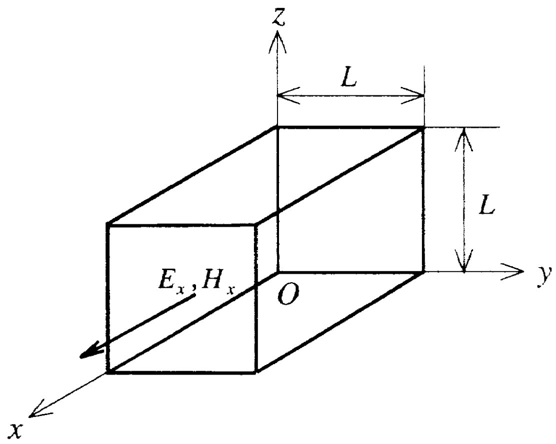

Fig. 1 Microcavity of square waveguide

The x−components E_x and H_x are perpendicular to each other and have the same eigenvalues k_{mn}, where $k_{mn} = \pi\sqrt{m^2+n^2}/L$.

Substituting $k_x = 2\pi/\lambda_p$ and $k_{mn} = 2\pi/\lambda_{mn}$ in Eq. (5), we obtain

$$\lambda_p = \frac{\lambda}{\sqrt{1-(\lambda/\lambda_{mn})^2}}, \qquad (6)$$

where λ_{mn} is called cut-off wavelength and λ_p guide wavelength. If $1-(\lambda/\lambda_{mn})^2 < 0$, i.e., $\lambda > \lambda_{mn}$, λ_p disappears. When λ_{mn} is λ_{10} or λ_{01}, it is $2L$ of the maximum wavelength. Therefore $\lambda_c (= \lambda_{10}\, or\, \lambda_{01})$ is the maximum cut-off wavelength of λ_{mn} that can exist in the cavity. The radiation of λ_c is the transverse standing wave, so that it does not travel in the direction +x and can not be emitted out of the cavity. Undoubtedly the radiation, the wavelengths of which are longer than λ_c, is never allowed to be generated in the cavity. The radiation, the wavelength of which, λ_{mn}, is shorter than λ_c, moreover, can not be emitted out of the cavity, because the wave of the radiation is the transverse standing wave, the wavelength of which is obtained from Eq. (5),

$$\lambda_{mn} = \frac{2L}{\sqrt{m^2+n^2}}. \qquad (7)$$

3.2 The Microcavities of Cylindrical Waveguide

In the microcavity of cylindrical waveguide with radius r_0 as shown in Fig.2, we considered the electromagnetic waves traveling in the direction +x. Substituting Ψ_x for one component of the electromagnetic waves in cylindrical coordinates, (r, ϕ, x), the separation of variables gives

$$\Psi_x = \sum_m \sum_{k_x} R(r)\Phi(\phi)X(x), \qquad (8)$$

where

$$R(r) = C_m J_m(\beta r), \quad \Phi(\phi) = B_m \cos m\phi + B_m' \sin m\phi, \quad X(x) = A e^{-jk_x x}, \qquad (9)$$

and $J_m(\beta r)$ is the Bessel function;

$$\beta = \sqrt{k^2 - k_x^2}. \qquad (10)$$

Analyzing Eq. (8), we obtain the E_x and H_x.

The x-component E_x is given by

$$E_x = E_{0x} J_m\left(P_{mn}\frac{r}{r_0}\right)\cos m\phi\, e^{-jk_x x}, \qquad (11)$$

where P_{mn} is the n th root of the $J_m(\beta r)$ and

$$\lambda_{mn} = (2\pi/p_{mn})r_0, \quad \lambda_p = \frac{\lambda}{\sqrt{1-(\lambda/\lambda_{mn})^2}}. \qquad (12)$$

The x-component H_x is given by

$$H_x = H_{0x} J_m\left(P_{mn}'\frac{r}{r_0}\right)\cos m\phi\, e^{-jk_x x}, \qquad (13)$$

where P_{mn}' is the n th root of the $J_m'(\beta r)$ and

$$\lambda_{mn} = (2\pi/p_{mn}')r_0, \quad \lambda_p = \frac{\lambda}{\sqrt{1-(\lambda/\lambda_{mn})^2}}. \qquad (14)$$

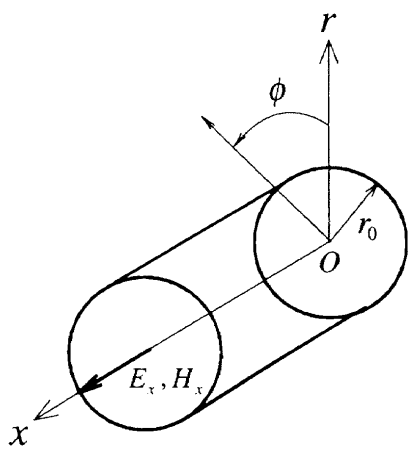

Fig. 2 Microcavity of cylindrical waveguide

4. The Skin Depth of the Cavity Walls

The conductivity, σ, of conventional metals such as tungsten is larger than the product $\omega\varepsilon$ within the wavelength range of electric waves, because ω, i.e., ν is low. The analysis of modes in the Sec. 2 can be applicable in this case, because the electromagnetic waves are almost perfectly reflected back into the cavity from the cavity walls and do not penetrate into them.

The conductivity, σ, however, is not as large as $\omega\varepsilon$, if ν is as high as, or higher than, the frequency of visible light. In that case we must analyze the modes taking into account the depth of penetration, i.e., the skin depth of cavity walls, because the electromagnetic waves penetrate into the cavity walls.

We evaluated the effect that the skin depth exerts an influence on the modes of electromagnetic waves in the microcavities. With Maxwell's third equation, the electric field, $\mathbf{E}$, in the cavities is described as follows:

$$\nabla\times\nabla\times\mathbf{E} = -\mu_0\varepsilon_0\frac{\partial^2\mathbf{E}}{\partial t^2}. \quad (15)$$

If we expand $\mathbf{E}$ and $\nabla\times\nabla\times\mathbf{E}$ using normalized eigenfunction, $\{\mathbf{F}_n\}$,

$$\mathbf{E} = \sum a_n(t)\mathbf{F}_n, \quad \nabla\times\nabla\times\mathbf{E} = \sum b_n(t)\mathbf{F}_n, \quad (16)$$

and

$$b_n = -\mu_0\varepsilon_0\frac{d^2a_n}{dt^2}, \quad a_n = \int_V \mathbf{F}_n^*\cdot\mathbf{E}dV, \quad b_n = \int_V \mathbf{F}_n^*\cdot\nabla\times\nabla\times\mathbf{E}dV, \quad (17)$$

where $\mathbf{F}_n^*$ is the nth conjugate complex number for $\mathbf{F}_n$. From the vector analysis on the parameter a_n, we obtain

$$\mu_0\varepsilon_0\frac{d^2a_n}{dt^2} + k_n^2a_n = -k_n^2\int_S(\mathbf{E}\times\mathbf{G}_n^*)\cdot\mathbf{n}dS \quad (18)$$

where G_n^* is the nth conjugate complex number for $\mathbf{G}_n$ and $\mathbf{G}_n = \nabla\times\mathbf{F}_n/k_n$.

4.1 The Cavities with the Walls of Perfect Conductors

In this case

$$\mu_0\varepsilon_0\frac{d^2a_n}{dt^2} + k_n^2a_n = 0, \quad (19)$$

because $\mathbf{n}\times\mathbf{E} = 0$ on the walls. Analyzing this equation, we obtain

$$\omega = \frac{k_n}{\sqrt{\mu_0\varepsilon_0}} = \omega_n \quad (20)$$

and, from Eq. (16), $\mathbf{E}$ is expressed as

$$\mathbf{E} = \sum A_n e^{j\omega_n t}\mathbf{F}_n, \quad (21)$$

because every mode is independent of each other, and we obtain, on the m th mode,

$$\mathbf{E}_m = a_m\mathbf{F}_m, \quad \mathbf{H}_m = j\frac{1}{\omega_m\mu_0}\nabla\times\mathbf{E}_m = ja_m\frac{\mathbf{G}_m}{Z_0}, \quad (22)$$

where $Z_0 = \sqrt{\mu_0/\varepsilon_0}$; Z_0 is the characteristic impedance of free space.

Therefore $\mathbf{H}$ can be expanded as follows:

$$\mathbf{H} = \sum\mathbf{H}_n = j\frac{1}{Z_0}\sum a_n\mathbf{G}_n. \quad (23)$$

4.2 The Cavities with the Walls of Imperfect Conductors

In this case, we obtain, on the mth mode of $(\mathbf{E}\times\mathbf{G}_m^*)\cdot\mathbf{n}$ in Eq. (18),

$$(\mathbf{E}\times\mathbf{G}_m^*)\cdot\mathbf{n} = \mathbf{G}_m^*\cdot(\mathbf{n}\times\mathbf{E}) = Z(\mathbf{H}\cdot\mathbf{G}_m^*), \quad (24)$$

because $\mathbf{n}\times\mathbf{E} = Z\mathbf{H}$ on the walls, S, where Z is the characteristic impedance of walls and $Z = \sqrt{\mu/(1-j\sigma/\omega)}$.

Even if $Z_0 \neq 0$, $\mathbf{H}$ can be replaced with $\mathbf{H}$ of Eq. (23) for approximation provided $Z << Z_0$; in this case, $Z = \sqrt{j\omega\mu/\sigma}$ and $\delta = \sqrt{2/\omega\mu\sigma}$, where δ is the skin depth of walls. Since $\mu \approx \mu_0$ on the conductors of non-magnetic material, we obtain, on the m th mode,

$$\mu_0\varepsilon_0\frac{d^2a_m}{dt^2} + k_m^2a_m = -j(1+j)(k_m^2\frac{\delta}{2}\int_S|\mathbf{G}_m|^2dS)a_m. \quad (25)$$

Now If we let L present the size of cavities, where L is the side of a cube or the diameter of a sphere, Eq. (25) becomes

$$\frac{d^2a_m}{dt^2} + \omega_m^2\left[1 - j(1-j)\frac{\delta}{L}\right]a_m = 0. \quad (26)$$

Analyzing this equation, we obtain

$$\omega = \omega_m\left[1-(1-j)\frac{\delta}{L}\right]^{\frac{1}{2}} \quad (27)$$

Provided $\delta/L << 1$, we obtain

$$\omega \approx \omega_m\left(1-\frac{\delta}{2L}\right) + j\omega_m\frac{\delta}{2L}. \quad (28)$$

Substitution of λ for ω and λ_m for ω_m gives

$$\lambda \approx \frac{\lambda_m}{1-\frac{\delta}{2L}} \approx \left(1+\frac{\delta}{2L}\right)\lambda_m \quad (29)$$

The conclusion of our analysis is that the resonance wavelength λ in the cavity with walls of the imperfect conductor of skin depth δ is longer than the resonance wavelength λ_0 in that with those of the perfect conductor by $(\delta/2L)\lambda_0$, i.e., the wavelength of electromagnetic waves resonating between the imperfect conductive walls with the skin depth δ and a separation L equals that of those resonating between the perfect conductive walls with the separation $[1+(\delta/2L)]L$.

5. The Skin Depth of Tungsten

The motion equation of the free electrons in metals under the action of the $\mathbf{E}$-field of electromagnetic waves, $\mathbf{E} = |\mathbf{E}|e^{j\omega t}$, is given as follows:

$$m\ddot{\mathbf{r}} + m\gamma\dot{\mathbf{r}} = e\mathbf{E}, \quad \gamma = 1/\tau, \tag{30}$$

where m is the mass of electron, e the charge of electron, τ the relaxation time, and $\mathbf{r}$ the position vector. Analyzing this equation, we obtain

$$\sigma = \frac{\sigma_0}{1+\omega^2\tau^2}, \tag{31}$$

where σ_0 is the conductivity when $\omega \to 0$. From the law of reflection and penetration on the electromagnetic waves, we obtain

$$\frac{4Z_0 Z}{(Z_0+Z)^2} = \kappa, \tag{32}$$

where κ is the emissivity. Substitution of $\eta = Z/Z_0$ gives

$$\varepsilon = \sqrt{\left(\frac{\varepsilon_0}{\eta^2}\right)^2 - \left(\frac{\sigma}{\omega}\right)^2}, \tag{33}$$

where

$$\eta = \left(\frac{2}{\kappa}-1\right) - \sqrt{\left(\frac{2}{\kappa}-1\right)^2 - 1}. \tag{34}$$

With ω, $\mu \approx \mu_0$, σ and ε, the skin depth is given by

$$\delta = \frac{\sqrt{2/\omega^2\mu_0\varepsilon}}{\sqrt{\sqrt{\left(\frac{\sigma}{\omega\varepsilon}\right)^2+1}-1}}. \tag{35}$$

Fig.3 shows an example where the skin depth of tungsten is calculated with a value of emissivity measured by De Vos[4]. The shorter the wavelength, the deeper the skin depth in the range of wavelength from visible to near ultraviolet light, as shown in Fig.3. The skin depth of tungsten at 2000k is about 83 nm at the cut-off wavelength of 700nm.

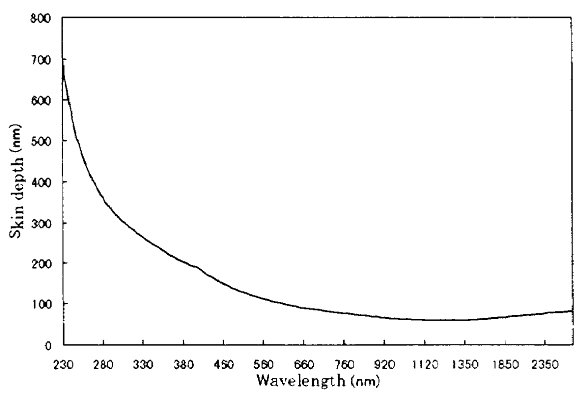

Fig. 3 Spectral distribution of the skin depth of tungsten

6. Radiant Emittance From the Microcavities

With the Fresnel-Kirchhoff diffraction formula, the spectral radiant emittance from cavities is given by

$$M_{MC}(\lambda,T) = \frac{c}{4}U_e(\lambda,T)\sqrt{1-\left(\frac{\lambda}{\lambda_c}\right)^2}, \tag{36}$$

where c is the light-velocity in free space and T is the absolute temperature of cavities. The function $U_e(\lambda,T)$, which is the spectral energy density of electromagnetic waves, can be described by Planck's radiation law,

$$U_e(\lambda,T) = \frac{8\pi hc}{\lambda^5}\cdot\frac{1}{e^{hc/\lambda kT}-1}d\lambda, \tag{37}$$

where h is Planck's constant and k is Boltzmann's constant.

7. The Spectral Radiant Emittance and Luminous Efficacy

Fig.4 shows examples of the spectral radiant emittance from microcavities. The spectral radiant emittance is evaluated provided the following condition:

(1) the cavities are vacuous,
(2) the cavity walls are tungsten,
(3) the temperature in cavities is 2000 K,
(4) the maximum cut-off wavelength is 700 nm.

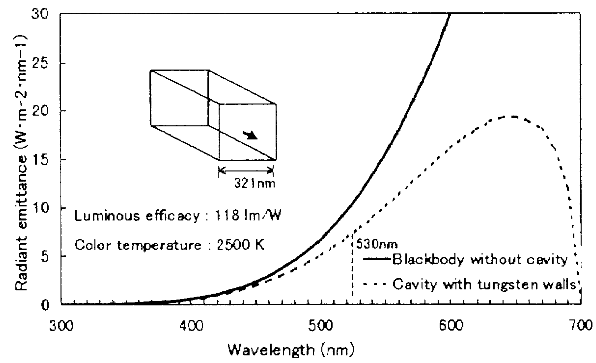

(1)A square microcavity

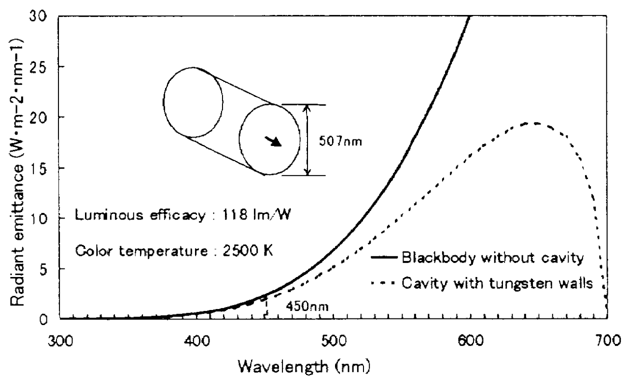

(2)A cylindrical microcavity

Fig. 4 Spectral radiant emittance from the microcavities

8. Conclusion

The modes of electromagnetic waves in the microcavities have been analyzed.. The skin depth of microcavity walls affects the mode of electromagnetic waves in the microcavities, so that it is the most important factor for a microcavity radiators. The skin depth of tungsten has been analyzed and then the spectral radiant emittance and luminous efficacy of radiation from the tungsten microcavities have been evaluated.

The skin depth of tungsten can be evaluated as about 83 nm at the cut-off wavelength of 700 nm and the luminous efficacy of radiation from the microcavity with that of 700 nm can be evaluated as about 118 lm/W.

More theoretical analysis of maicrocavity radiators is left as a future work.

References

(1) Waymouth, J. F. : Where will the Next Generation of Lamps Come from?, J. Light & Vis. Env., Vol. 13, No.2, pp.51-68 (1989).

(2) SUGIMOTO, M., FUJIOKA, T., INOUE, T., FUKUSIMA,H., MIZUYAMA,Y., UKEGAWA, S., MATSUSIMA,T., TOHO, M. : The Infra-red Suppression in the Incandescent Light from a Surface with Submicron Holes, J. Light & Vis. Env., Vol.18, No.2, pp.5-9 (1994).

(3) SHIBATA,T., SAKURAOKA,T., SEKI,M., OHKAWA,M., SEKINE,S. : Study on radiators reducing the emissivity in the infra-red wavelength, Proceedings of 1995 Annual Conference of the Illuminating Engineering Institute of Japan, p.47(1995).

(4) De Vos.,J.C. : A new determination of the emissivity of tungsten ribbon, Physica [Holland],Vol.20, pp.690-714 (1954).